Solid-state reaction mechanism for the formation of $Ba_{6-x}Ln_{8+2x/3}Ti_{18}O_{54}$ (Ln = Nd, Sm) solid solutions

Anatolii G. Belous and Oleg V. Ovchar
V.I. Vernadskii Institute of General and Inorganic Chemistry of Ukrainian National Academy of Sciences, Kiev, Ukraine

Matjaz Valant and Danilo Suvorov
"Jozef Stefan" Institute, Ljubljana, Slovenia

(Received 20 March 2000; accepted 29 May 2001)

A solid-state reaction mechanism for the formation of $Ba_{6-x}Ln_{8+2x/3}Ti_{18}O_{54}$ (Ln = Nd, Sm) solid solutions has been studied using x-ray powder diffraction, thermal analyses, and transmission electron microscopy (TEM). During the interaction of the starting reagents, $Ln_2Ti_2O_7$, $BaTi_4O_9$, and $BaTiO_3$ are formed. In the next sequence, these three phases react together to form a high-x end member of the $Ba_{6-x}Ln_{8+2x/3}Ti_{18}O_{54}$ homogeneity region ($Ba_{3.9}Nd_{9.4}Ti_{18}O_{54}$ and $Ba_{3.9}Sm_{9.4}Ti_{18}O_{54}$). Subsequently, the reaction of $Ba_{3.9}Nd_{9.4}Ti_{18}O_{54}$ and $Ba_{3.9}Sm_{9.4}Ti_{18}O_{54}$ with the residual $BaTiO_3$ takes place. TEM investigations revealed that compositional inhomogeneities and structural defects existed in the $Ba_4Sm_{9.33}Ti_{18}O_{54}$ sample heated at 1370 °C for 1 h. Sintering times, prolonged to $\geqslant$3 h, eliminated the structural defects and increased the homogeneity of the sample.

I. INTRODUCTION

The recent development of wireless-communication systems operating in the microwave-frequency range has created a need for ceramic materials with high, temperature-stable, permittivity and low dielectric losses to be used as oscillating or filtering devices (local oscillators, microwave filters) or as dielectric substrates. The effective size of these components decreases with increasing permittivity (ϵ) of the material, which makes high-permittivity materials (ϵ = 80–100) such as $Ba_{6-x}Ln_{8+2x/3}Ti_{18}O_{54}$ (Ln = La–Gd) very attractive. Recently, the main emphasis has been given to decreasing the dielectric loss to enhance the frequency selectivity of the components.[1–3] Neodymium and samarium analogues of the $Ba_{6-x}Ln_{8+2x/3}Ti_{18}O_{54}$ solid solutions are of special interest because of their potential applications such as dielectric resonators and filters. The neodymium analogue is characterized by a positive value of temperature coefficient of resonant frequency (τ_f) while samarium-containing materials have slightly negative τ_f at operating temperatures.[4] In both cases, τ_f can be suppressed by a small modification to the stoichiometry or phase composition, without significant deterioration of the dielectric losses.[5]

The crystal structure of $Ba_{6-x}Ln_{8+2x/3}Ti_{18}O_{54}$ solid solutions includes elements of the tungsten-bronze structure with channels extending in the short-axis direction.[6–8] Corner-sharing TiO_6 octahedra form a network with three types of channels: pentagonal; rhombic; triangular. Rare-earth ions occupy the rhombic channels, Ba ions completely fill the pentagonal channels (for $x < 2$), and the remaining Ba ions share the rhombic channels. The triangular channels are empty. The homogeneity region of the Nd analogue extends in the range of $0 < x < 2.1$[9] or $0.6 < x < 2.1$,[4] whereas for the Sm analogue the range is $0.6 < x < 2.1$.[4,9]

Only a few studies concerning the formation of $Ba_{6-x}Ln_{8+2x/3}Ti_{18}O_{54}$ solid solutions can be found in the literature[10,11] although understanding of the reaction mechanisms and kinetics can be crucial for the suppression of extrinsic dielectric losses. These kinds of losses appear in single-phase $Ba_{6-x}Ln_{8+2x/3}Ti_{18}O_{54}$ ceramics as a result of compositional inhomogeniety and a high concentration of structural defects. The published studies performed for the coprecipitated starting powder[10] or starting powder with an excess of TiO_2[11] disclosed some major reaction sequences. However, details on the formation of the final $Ba_{6-x}Ln_{8+2x/3}Ti_{18}O_{54}$ composition that crucially influence dielectric losses were not revealed. Therefore, the goal of this study was to investigate the formation sequences of the solid-state synthesis of the $Ba_{6-x}Ln_{8+2x/3}Ti_{18}O_{54}$ solid solution (Ln = Sm, Nd) over the entire homogeneity range. On the basis of these results, the critical stages of the thermal processing were exposed which could efficiently optimize the firing conditions and reduce the resulting dielectric losses of the samples fabricated.

II. EXPERIMENTAL

The solid-state reaction mechanisms for $Ba_{6-x}Ln_{8+2x/3}Ti_{18}O_{54}$ (Ln = Nd, Sm) were examined for the compositions $x = 0.75$, 1.5, and 2.0. Reagent-grade powders of Sm_2O_3, Nd_2O_3 and TiO_2, with a particle size of approximately 0.5 μm, and $BaCO_3$, with a particle size of approximately 1 μm, were used as starting reagents. The starting reagents were mixed in the stoichiometric ratio and ball-milled for 4 h in water using agate bowls. The mixture blend was dried and then pressed under a pressure of 500 kg/cm^2. The resulting preforms were prereacted at 800–1400 °C for 4 h, quenched to room temperature, and crushed to produce homogeneous powders. The products obtained were analyzed by powder x-ray diffraction (XRD) analysis (DRON-3M) using Cu K_α radiation.

Phase composition analysis and elementary microanalysis of the sintered samples were performed by scanning electron microscopy (JEOL, JSM 5800, Tokyo, Japan) using energy dispersive x-ray spectroscopy (EDX) and the LINK software package (ISIS 3000, Oxford Instruments, Bucks, UK). To verify the chemical

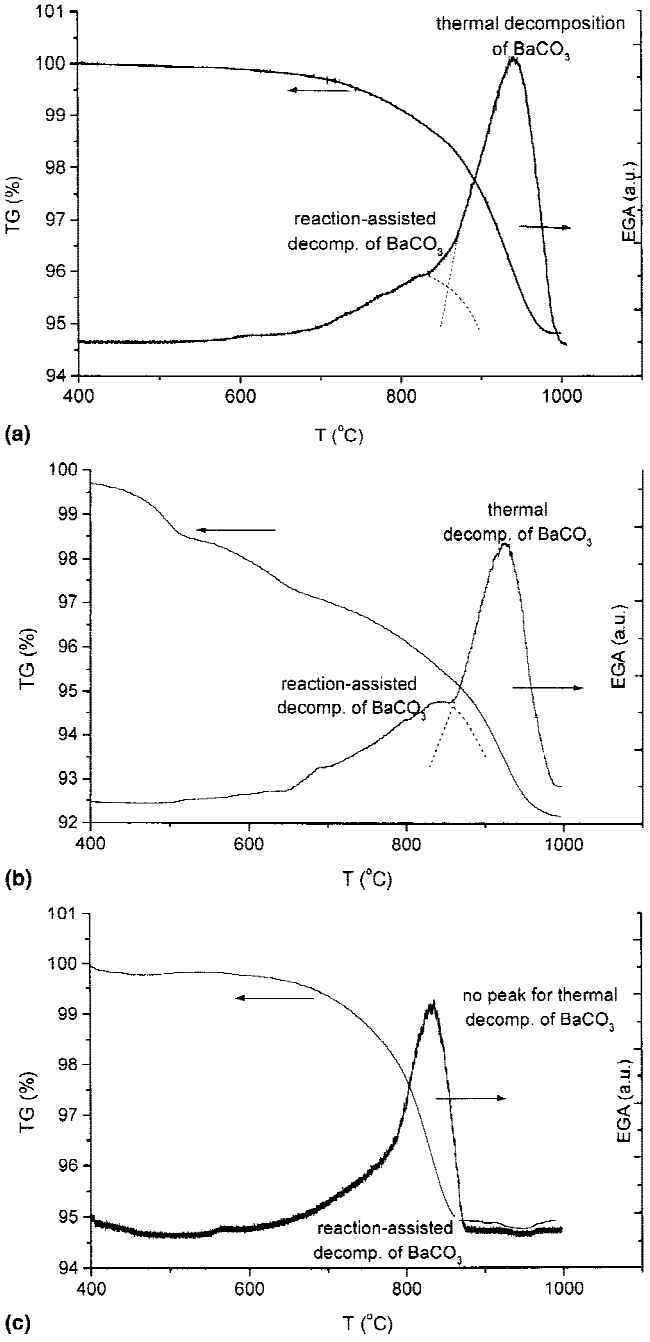

FIG. 1. Thermogravimetric analyses and evolved gas analyses of 5.25 $BaCO_3$–4.25 Nd_2O_3–18 TiO_2 mixture [heating time (a) 5 °C/min, (b) 2 °C/min, and (c) 0.5 °C/min].

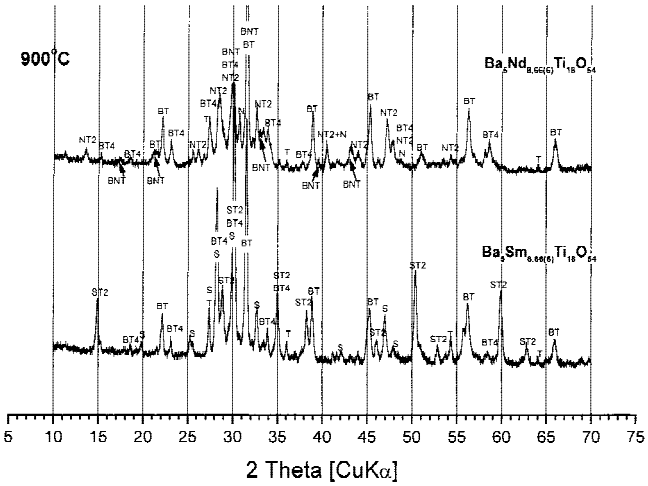

FIG. 2. XRD patterns of the reaction mixtures with the initial compositions corresponding to $Ba_{6-x}Nd_{8+2x/3}Ti_{18}O_{54}$ ($x = 0.75$) and $Ba_{6-x}Sm_{8+2x/3}Ti_{18}O_{54}$ ($x = 0.75$) quenched from 990 °C. (For phase denotation, see Table I.)

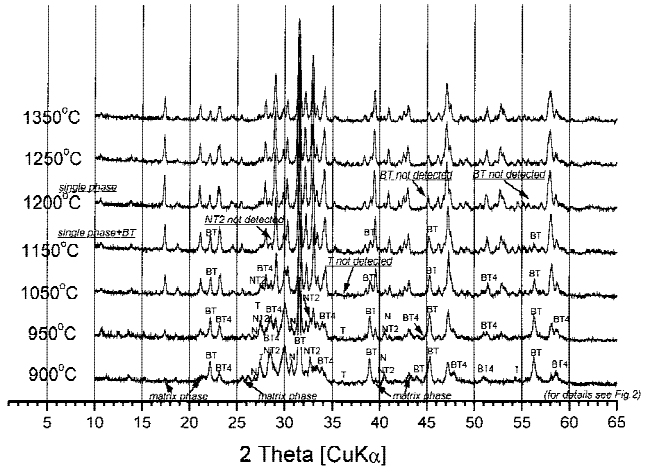

FIG. 3. XRD patterns of the reaction mixture with the initial composition corresponding to $Ba_{6-x}Nd_{8+2x/3}Ti_{18}O_{54}$ ($x = 0.75$) quenched from different temperatures (900 to 1350 °C). (For phase denotation, see Table I.)

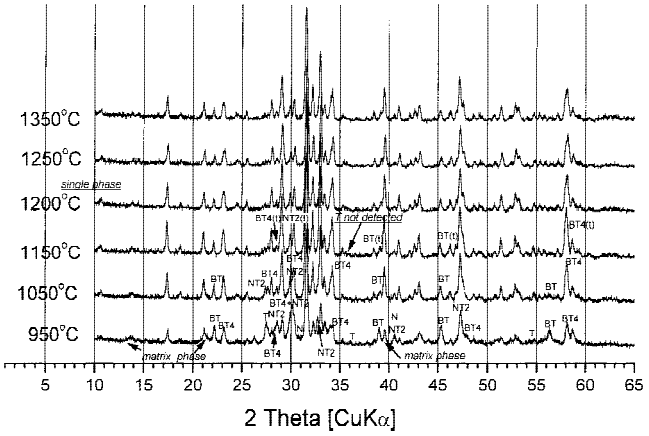

FIG. 4. XRD patterns of the reaction mixture with the initial composition corresponding to $Ba_{6-x}Nd_{8+2x/3}Ti_{18}O_{54}$ ($x = 2.0$) quenched from different temperatures (950 to 1350 °C). (For phase denotation, see Table I.)

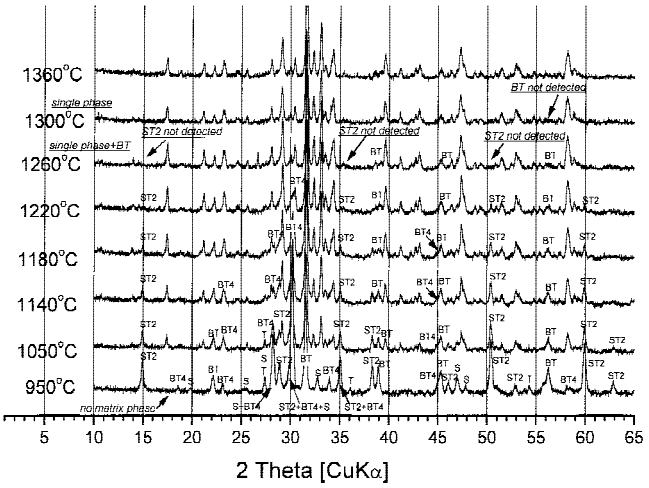

FIG. 5. X-ray diffraction patterns of the reaction mixture with the initial composition corresponding to $Ba_{6-x}Sm_{8+2x/3}Ti_{18}O_{54}$ ($x = 0.75$) quenched from different temperatures (950 to 1360 °C). (For phase denotation, see Table I.)

composition of the synthesized single-phase powders the samples were fused with borax or potassium pyrosulfate and dissolved in sulfuric acid. The rare-earth elements content was determined by complexometric titration with EDTA and xylenol orange in a light acidic solution. The barium content was determined by weight methods, and the titanium content was determined by colorimetry. The total uncertainty of the element determination was 0.5–1.0%.

Ceramics for transmission electron microscopy (TEM) analyses were produced from the powder, prereacted at 1150 °C, and fired at 1370 °C for 1 to 4 h. Foils were prepared by argon-ion erosion at 4 kV with an incident angle of about 10° using a dimple grinder (GATAN, Gatan, Inc., Warrendale, PA). Electron diffraction studies and microscopic investigations of the foils were performed using a transmission electron microscope (JEOL 2000FX, JEOL, Tokyo, Japan) operating at 200 kV. Thermogravimetric analyses (TG) were carried out with a STA 409 Netzsch system in the air with Pt crucible and heating rates of 5 and 0.5 °C/min. Evolved gas analyses (EGA) were performed on a CO_2^+ fragment with a quadropol mass spectrometer (Thermostar GSD 300T Baltzers, Baltzers Instruments, Liechenstein).

III. RESULTS AND DISCUSSION

XRD patterns of the reaction products obtained by interrupting the reaction at certain temperatures were analyzed to ascertain the reaction sequence. It was evident from these patterns that formation of the final product phase often began before the entirety of the starting reagents was consumed in the formation of intermediate phases. That is to say, due to kinetic reasons, various reaction steps overlapped, and thus, the following description of the reaction sequence is necessarily simplified.

TABLE I. Phase composition (determined by x-ray analyses) of the reaction mixture quenched from different temperatures. Initial composition corresponds to $Ba_{6-x}Nd_{8+2x/3}Ti_{18}O_{54}$ ($x = 0.75$), $Ba_{6-x}Nd_{8+2x/3}Ti_{18}O_{54}$ ($x = 2.0$), and $Ba_{6-x}Sm_{8+2x/3}Ti_{18}O_{54}$ ($x = 0.75$).

$Ba_{6-x}Nd_{8+2x/3}Ti_{18}O_{54}$ ($x = 0.75$)		$Ba_{6-x}Nd_{8+2x/3}Ti_{18}O_{54}$ ($x = 2.0$)		$Ba_{6-x}Sm_{8+2x/3}Ti_{18}O_{54}$ ($x = 0.75$)	
T_q (°C)[a]	Phase composition[a]	T_q (°C)[a]	Phase composition[a]	T_q (°C)[a]	Phase composition[a]
900	N, T, BT, BT4, NT2, BNT(t)			900	S, T, BT, BT4, ST2
950	N(t), T, BT, BT4, NT2, BNT	950	N(t), T, BT, BT4, NT2, BNT	950	S, T, BT, BT4, ST2
1050	BT, BT4(t), NT2, BNT	1050	BT, BT4, BNT	1050	T(t), BT, BT4, ST2, BST
1150	BT, BNT	1150	BT(t), BT4(t), BNT	1140	BT, BT4, ST2, BST
1200	BNT	1200	BNT	1180	BT, BT4, ST2, BST
1250	BNT	1250	BNT	1220	BT, BT4, ST2, BST
1350	BNT	1350	BNT	1260	BT, BST
				⩾1300	BST

[a]N = Nd_2O_3, S = Sm_2O_3, T = TiO_2, BT = $BaTiO_3$, BT4 = $BaTi_4O_9$, NT2 = $Nd_2Ti_2O_7$, ST2 = $Sm_2Ti_2O_7$, BNT = $Ba_{6-3x}Nd_{8+2x/3}Ti_{18}O_{54}$, BST = $Ba_{6-3x}Sm_{8+2x}Ti_{18}O_{54}$, t = faint diffraction peak indicates small concentration of the phase, and T_q = quenching temperature.

A. Reactions of the starting reagents

The first interaction between starting reagents occurs in the temperature range from 800 to 950 °C. Although pure $BaCO_3$ starts dissociating in air at >900 °C,[12] results of the thermal analyses showed that during the firing of the $BaCO_3$–Ln_2O_3–TiO_2 starting mixture, CO_2 was released much earlier (Fig. 1) The EGA curves, taken with heating rates of 5 and 2 °C/min, show two peaks corresponding to the release of CO_2. Some of the CO_2 is released during the initial reaction of $BaCO_3$ with other oxides present at temperatures from 700 to 850 °C. The small EGA peak is followed by a much larger peak above 900 °C, which reveals the direct thermal decomposition of $BaCO_3$. The same TG-EGA experiment was repeated with a slower heating rate of 0.5 °C/min. In this case, the second EGA peak disappeared indicating all the $BaCO_3$ reacted with oxides below 900 °C.

The EGA experiments suggest that either TiO_2 reacts with $BaCO_3$ to form $BaTiO_3$ directly or, alternatively, TiO_2 (or Ln_2O_3) only catalyzes the dissociation of $BaCO_3$ and subsequently reacts with the transient BaO phase to form $BaTiO_3$. On the basis of the experimental result, we could not discriminate between these two possibilities. Nevertheless, the formation of $BaTiO_3$ at 900 °C is clearly evident from x-ray analyses (Fig. 2).

Another reaction that took place below 1000 °C is the reaction of TiO_2 with a rare earth to produce $Ln_2Ti_2O_7$. Not all of the TiO_2 is consumed for the formation of $BaTiO_3$ and $Ln_2Ti_2O_7$, but some TiO_2 reacted with $BaTiO_3$. As shown by Templeton and Pask,[12] the reaction of $BaTiO_3$ and TiO_2 is diffusion controlled and can give different barium polytitanate species. From the x-ray patterns it was evident that $BaTi_4O_9$ was predominantly formed, while no other barium polytitanates were detected. Significant concentrations of other polytitanates (e.g., $Ba_4Ti_{13}O_{30}$) were detected by Wu *et al.*[11] when they started the synthesis from a nonstoichiometric mixture.

The reactions of the starting reagents are mostly completed at 1050 °C, and only traces of the starting reagents can still be seen in an x-ray pattern (Figs. 3–5). The reaction sequence of starting reagents can be written as proposed below. The reaction coefficients were calculated from the balance of the reaction and are given corresponding to the stoichiometry for $Ba_{6-x}Ln_{8+2x/3}Ti_{18}O_{54}$ with $x = 0.75$ and in parentheses with $x = 2.1$ (a low Ba end member within the homogeniety range of Nd and Sm analogues).

$$5.25(3.90)BaCO_3 + 5.25(3.90)TiO_2 \rightarrow 5.25(3.90)BaTiO_3 + 5.25(3.90)CO_2 \quad , \tag{1}$$

$$4.25(4.70)Ln_2O_3 + 8.50(9.40)TiO_2 \rightarrow 4.25(4.70)Ln_2Ti_2O_7 \quad , \tag{2}$$

$$1.42(1.56)BaTiO_3 + 4.25(4.7)TiO_2 \rightarrow 1.42(1.56)BaTi_4O_9 \quad . \tag{3}$$

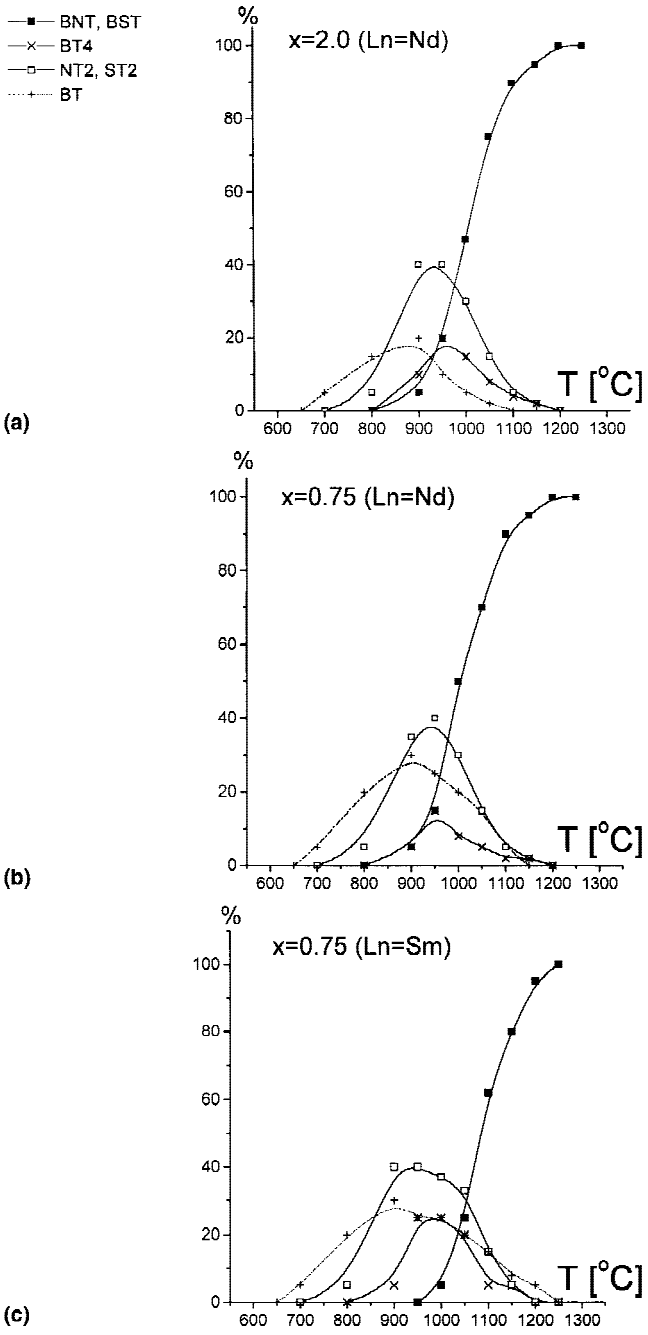

FIG. 6. Phase fraction as a function of calcination temperature for mixtures with the nominal compositions. $Ba_{6-x}Nd_{8+2x/3}Ti_{18}O_{54}$ (a) $x = 0.75$ and (b) $x = 2.0$ and (c) $Ba_{6-x}Sm_{8+2x/3}Ti_{18}O_{54}$ $x = 0.75$. (For phase denotation, see Table I.)

After the completion of reactions (1)–(3) the reaction mixture consists of $4.25(4.70)Ln_2Ti_2O_7$, $1.42(1.56)BaTi_4O_9$, and $3.83(2.34)BaTiO_3$.

B. Reaction of $Ln_2Ti_2O_7$

The binary compounds present in the reaction mixture, $Ln_2Ti_2O_7$, $BaTi_4O_9$, and $BaTiO_3$, start reacting to form the $Ba_{6-x}Ln_{8+2x/3}Ti_{18}O_{54}$ phase at approximately 900

and 1050 °C for the Nd and Sm analogue, respectively (Table I). X-ray analysis showed that the reaction sequence for all three systems studied ($Ba_{5.25}Nd_{8.5}Ti_{18}O_{54}$, $Ba_4Nd_{9.33}Ti_{18}O_{54}$, $Ba_{5.25}Sm_{8.5}Ti_{18}O_{54}$) was the same. The concentration of the matrix $Ba_{6-x}Ln_{8+2x/3}Ti_{18}O_{54}$ phase increases with temperature while the amount of $Ln_2Ti_2O_7$ and $BaTi_4O_9$ decreases at a similar rate for all *x*. The decrease in the concentration of $BaTiO_3$ with the temperature is not unaffected by *x* (Fig. 6). and is higher for high-*x* than for low-*x* compositions. Moreover, for both low-*x* compositions a temperature exists (1200 and 1260 °C for the Nd and Sm analogues, respectively) where only two phases, $Ba_{6-x}Ln_{8+2x/3}Ti_{18}O_{54}$ and $BaTiO_3$, are present in the reaction mixture. For the high-*x* composition sample, no such range was observed. The variations in the amount of $BaTiO_3$ indicated that, during the reaction of $Ln_2Ti_2O_7$, $BaTi_4O_9$, and $BaTiO_3$, the high-*x* end members of the $Ba_{6-x}Ln_{8+2x/3}Ti_{18}O_{54}$ solid solutions, $Ba_{3.9}Nd_{9.4}Ti_{18}O_{54}$ and $Ba_{3.9}Sm_{9.4}Ti_{18}O_{54}$, are formed first [according to reaction (4)] and, subsequently, the reaction of the high-*x* $Ba_{6-x}Ln_{8+2x/3}Ti_{18}O_{54}$ with the remaining $BaTiO_3$ follows:

$$4.25(4.70)\ Ln_2Ti_2Ti_2O_7 + 1.42(1.56)BaTi_4O_9 + 3.83(2.34)BaTiO_3 \rightarrow 0.90(1.00)Ba_{3.9}Ln_{9.4}Ti_{18}O_{54} + 1.73(0.00)BaTiO_3 \quad . \qquad (4)$$

From the x-ray patterns it is not possible to determine unambiguously the detailed formation mechanism of the high-*x* end members of $Ba_{6-x}Ln_{8+2x/3}Ti_{18}O_{54}$. It might be expected that reaction (4) does not occur as written, as the simultaneous interaction of three phases, $Ln_2Ti_2O_7$, $BaTi_4O_9$, and $BaTiO_3$, but rather as a sequential interaction between two of those three phases. On the basis of this postulation, two alternative mechanisms can be assumed: (i) intermediate formation of a transient perovskite $Ln_{2/3}TiO_3$ phase, which was also reported by Takahashi *et al.*[10] (the instability of the $Ln_{2/3}TiO_3$ phases in their stoichiometric form necessitates the existence of an additional stabilizing mechanism, either the partial transient reduction of Ti^{4+} to Ti^{3+} or the incorporation of additional ions on the vacancy sites of the deficient $Ln_{2/3}TiO_3$ perovskite[13]), followed by the reaction with Ba–polytitanates or (ii) iterative reaction between $Ln_2Ti_2O_7$ and $BaTi_4O_9$ with the direct formation of $Ba_{3.9}Ln_{9.4}Ti_{18}O_{54}$. During this reaction, TiO_2 would be released and during the reaction with $BaTiO_3$ would form a $BaTi_4O_9$ phase, which might re-enter the reaction with the remaining $Ln_2Ti_2O_7$.

C. Formation of final $Ba_{6-x}Ln_{8+2x/3}Ti_{18}O_{54}$ composition

After the completion of the reactions implied by Eq. (4), only two phases, $Ba_{3.9}Ln_{9.4}Ti_{18}O_{54}$ and $BaTiO_3$, exist in the reaction mixture with the nominal composition of $x < 2.1$. They reacted with each other to form a final $Ba_{6-x}Ln_{8+2x/3}Ti_{18}O_{54}$ with intended composition.

$$0.90Ba_{3.9}Ln_{9.4}Ti_{18}O_{54} + 1.73BaTiO_3 \rightarrow 1.00\ Ba_{5.25}Ln_{8.5}Ti_{18}O_{54} \quad . \qquad (5)$$

The x-ray data showed that the perovskite $BaTiO_3$ phase completely disappeared at approximately 1250 and approximately 1300 °C for the Nd and Sm analogue, respectively, which apparently implied the formation of a single-phase compound. However, detailed TEM analyses revealed a certain degree of inhomogeniety in the sample. The TEM analyses of the samples with $x = 1.5$ sintered for 1 h at 1370 °C showed the presence of an additional phase appearing as an inclusion in the matrix

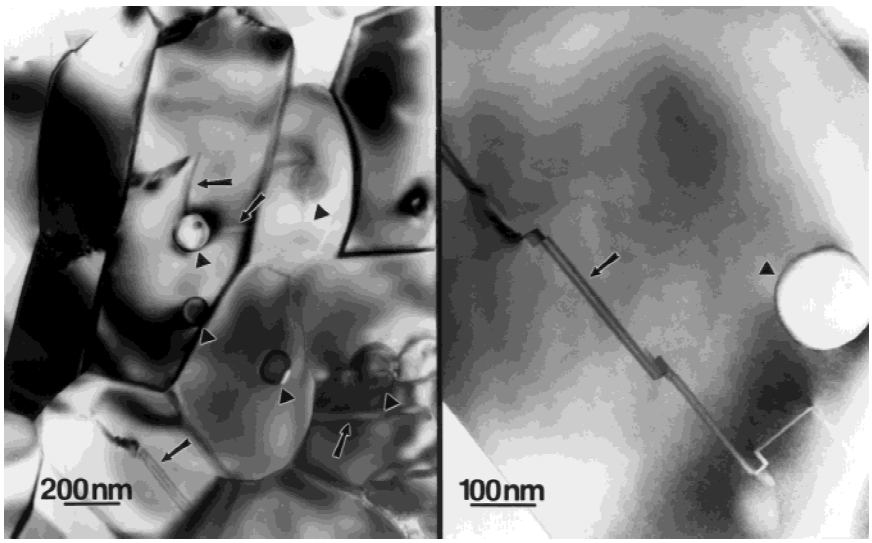

FIG. 7. TEM micrographs of the $Ba_{6-x}Sm_{8+2x/3}Ti_{18}O_{54}$ ($x = 1.5$) sample sintered for 1 h at 1370 °C showing an additional phase (triangles) and structural defects (arrows) in the matrix grains.

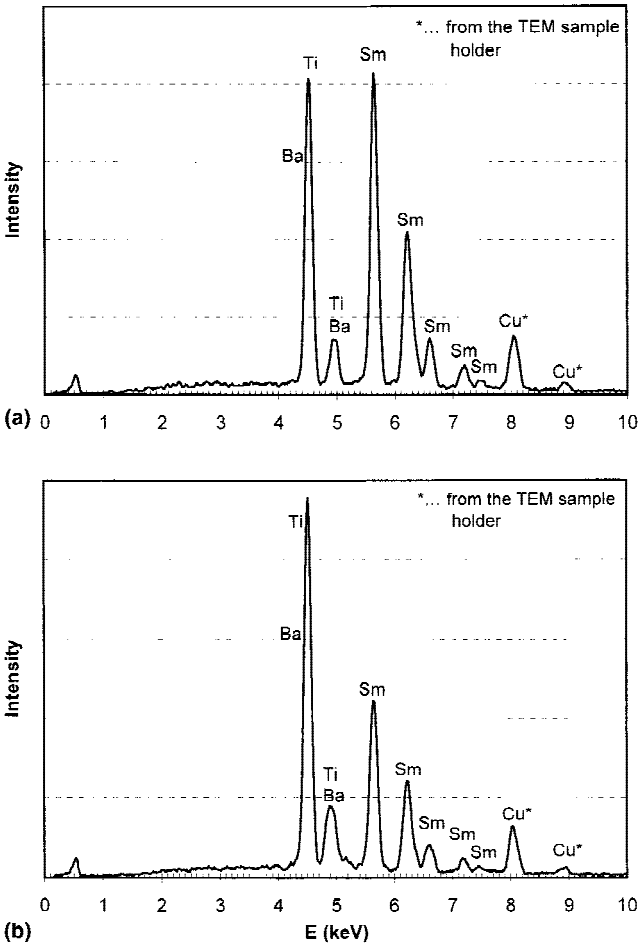

FIG. 8. Comparison of the EDS spectra of the (a) inclusions in the matrix grains and (b) matrix phase.

grain (Fig. 7). This is accompanied by a high concentration of 2-dimensional structural defects, mostly antiphase boundaries. In contrast, the concentration of the inclusions and defects was significantly lower for the samples with higher x values.

The EDS analyses on the inclusions showed that they were a ternary phase with a higher Sm content than that of the matrix (Fig. 8). The TEM analyses also showed that the concentration of inclusions and structural defects decreased with an increase in sintering time, as can be seen for the sample sintered for 4 h at 1370 °C in Fig. 9.

On the basis of the TEM analyses it might be concluded that the reaction between $Ba_{3.9}Ln_{9.4}Ti_{18}O_{54}$ and $BaTiO_3$ started on the surfaces of the $Ba_{3.9}Ln_{9.4}Ti_{18}O_{54}$ grains and proceeded with the diffusion of Ba and Ti ions into the grains. Even when all the $BaTiO_3$ reacted, phase equilibrium was still not necessarily achieved and the ceramics consisted of low- and high-x $Ba_{6-x}Ln_{8+2x/3}Ti_{18}O_{54}$ phases. Compositional homogeneity could be achieved after a prolonged sintering time leading to the formation of the final $Ba_{6-x}Ln_{8+2x/3}Ti_{18}O_{54}$ composition.

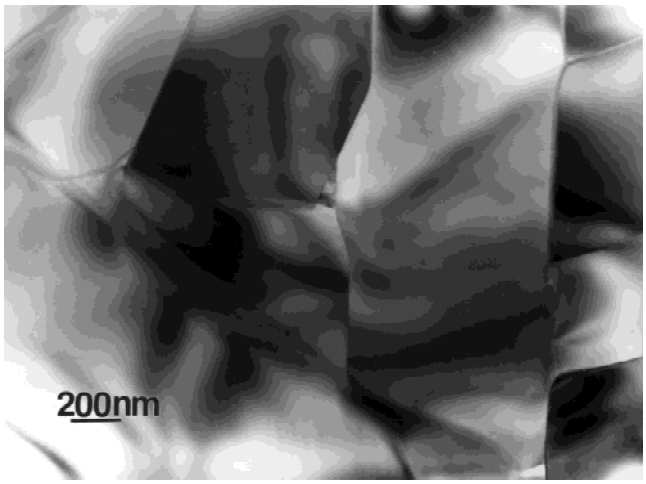

FIG. 9. TEM micrograph of the $Ba_{6-x}Sm_{8+2x/3}Ti_{18}O_{54}$ ($x = 1.5$) sample sintered for 3 h at 1370 °C showing no additional phase and no structural defects.

Regarding the dielectric properties, it is important to understand that the homogenous $Ba_{6-x}Ln_{8+2x/3}Ti_{18}O_{54}$ solid solution exhibits dielectric properties different from those of the composite ceramics consisting of two $Ba_{6-x}Ln_{8+2x/3}Ti_{18}O_{54}$ phases. This is due to the nonlinear change in the dielectric properties with x which is especially pronounced in the case of the Sm analogue.[4,9] The practical consequence of the results described is that the reproducibility for the dielectric properties of the $Ba_{6-x}Ln_{8+2x/3}Ti_{18}O_{54}$-based dielectric ceramics is strongly affected by the heat treatment conditions. Prolonged sintering times ($\geqslant$3 h) are recommended to eliminate structural defects and obtain complete homogenization of $Ba_{6-x}Ln_{8+2x/3}Ti_{18}O_{54}$.

IV. CONCLUSIONS

Formation of $Ba_{6-x}Ln_{8+2x/3}Ti_{18}O_{54}$ (Ln = Sm, Nd) solid solutions began with reactions between the starting reagents to yield the intermediate products $Ln_2Ti_2O_7$, $BaTi_4O_9$, and $BaTiO_3$. On the basis of the changes in the relative intensities of XRD peaks, it was revealed that during the interaction of the intermediate products, the high-x end members of the $Ba_{6-x}Ln_{8+2x/3}Ti_{18}O_{54}$ solid solutions were formed first ($Ba_{3.9}Nd_{9.4}Ti_{18}O_{54}$ and $Ba_{3.9}Sm_{9.4}Ti_{18}O_{54}$). Subsequently, these reacted with the residual $BaTiO_3$ to produce the intended $Ba_{6-x}Ln_{8+2x/3}Ti_{18}O_{54}$ composition. TEM investigations revealed that even when all the $BaTiO_3$ had reacted, compositional homogeneity was still not necessarily achieved. Ceramics sintered for a short period consisted of low- and high-x $Ba_{6-x}Ln_{8+2x/3}Ti_{18}O_{54}$ phases with a significant concentration of crystal-structure defects. The concentration of crystal-structure defects was suppressed and the compositional homogeneity of $Ba_{6-x}Ln_{8+2x/3}Ti_{18}O_{54}$ was improved after a prolonged sintering time ($\geqslant$3 h).

REFERENCES

1. K. Fukuda, I. Fujii, R. Kitoh, Y. Cho, and I. Awai, Jpn. J. Appl. Phys. **32,** 1712 (1993).
2. H. Ohsato, M. Imaeda, Y. Takagi, A. Komura, T. Okuda, and S. Nishigaki, edited by E. Colla and D. Damjanovic (Proc. 11th IEEE Int. Symp. Appl. Ferroelectr., Montreux, Switzerland, 1998), p. 509.
3. A.G. Belous, O.V. Ovchar, M. Valant, and D. Suvorov, Appl. Phys. Lett. **77,** 1707 (2000).
4. T. Negas and P.K. Davies, Ceram. Trans. **53,** 179 (1995).
5. D. Suvorov, M. Valant, and D. Kolar, J. Mater. Sci. **32,** 6483 (1997).
6. R.G. Matveeva, M.B. Varfolomev, and L.S. Il'yuhchenko, Russ. J. Inorg. Chem. **29,** 17 (1984).
7. F. Azough, P. Setaswuwon, and R. Freer, Ceram. Trans. **53,** 215 (1995).
8. C.J. Rawn, D.P. Birnie, M.A. Bruck, J.H. Enemark, and R.S. Roth, J. Mater. Res. **13,** 187 (1998).
9. H. Ohsato, T. Ohhashi, S. Nishigaki, T. Okuda, K. Sumia, and S. Suzuki, Jpn. J. Appl. Phys. **32,** 4323 (1993).
10. J. Takahashi, T. Ikegami, and K. Kageyama, J. Am. Ceram. Soc. **74,** 1868 (1991).
11. J.M. Wu, M.C. Chang, and P.C. Yao, J. Am. Ceram. Soc. **73,** 1599 (1990).
12. L.K. Templeton and J.A. Pask, J. Am. Ceram. Soc. **42,** 212 (1959).
13. M. Abe and K. Uchino, Mater. Res. Bull. **9,** 147 (1974).